



# Hierarchical silicon nanowires-carbon textiles matrix as a binder-free anode for high-performance advanced lithium-ion batteries

Bin Liu<sup>1</sup>, Xianfu Wang<sup>1</sup>, Haitian Chen<sup>3</sup>, Zhuoran Wang<sup>1</sup>, Di Chen<sup>1</sup>, Yi-Bing Cheng<sup>2</sup>, Chongwu Zhou<sup>3</sup> & Guozhen Shen<sup>1,4</sup>

<sup>1</sup>Wuhan National Laboratory for Optoelectronics (WNLO) and College of Optical and Electronic Information, Huazhong University of Science and Technology (HUST), Wuhan 430074, P. R. China, <sup>2</sup>Faculty of Engineering, Monash University, VIC 3800, Australia, <sup>3</sup>Department of Electric Engineering, University of Southern California, Los Angeles, California 90089, United States, <sup>4</sup>State Key Laboratory for Superlattices and Microstructures, Institute of Semiconductors, Chinese Academy of Sciences, Beijing 100083, P. R. China.

**Toward the increasing demands of portable energy storage and electric vehicle applications, the widely used graphite anodes with significant drawbacks become more and more unsuitable. Herein, we report a novel scaffold of hierarchical silicon nanowires-carbon textiles anodes fabricated via a facile method. Further, complete lithium-ion batteries based on Si and commercial LiCoO<sub>2</sub> materials were assembled to investigate their corresponding across-the-board performances, demonstrating their enhanced specific capacity (2950 mAh g<sup>-1</sup> at 0.2 C), good repeatability/rate capability (even >900 mAh g<sup>-1</sup> at high rate of 5 C), long cycling life, and excellent stability in various external conditions (curvature, temperature, and humidity). Above results light the way to principally replacing graphite anodes with silicon-based electrodes which was confirmed to have better comprehensive performances.**

Rechargeable lithium-ion batteries are fast-growing technology that is attractive for potential applications in portable electronics and electric vehicles due to their relatively high energy and power densities<sup>1-6</sup>. The currently commercial graphite anodes with the low theoretical capacity (372 mAh g<sup>-1</sup>) and poor rate capability can not satisfy the requirements of high-efficient next-generation energy storage systems<sup>7</sup>. Herein, the basic strategy has been performed in order to search for various lithium insertion metals as alternative anodes<sup>8,9</sup>. In particular, silicon has been proposed as one of the most promising anode materials due to its corresponding high theoretical lithium storage capacity (4200 mAh g<sup>-1</sup> for Li<sub>22</sub>Si<sub>5</sub>, 11.3 times that of commercial graphite), high volumetric capacity (9786 mAh cm<sup>-3</sup>), and low cost<sup>10-20</sup>. The major drawbacks are the volume expansion upon Li insertion of silicon itself due to the formation of Li<sub>x</sub>Si alloys that causes cracking and pulverization of Si particles as well as the fracture behavior and cracking patterns in amorphous Si film-electrode, thereby leading to the loss of electrical contact and short cycle life<sup>21-24</sup>. Commonly, coating graphite and decreasing the dimensions to one-dimension, and patterning the electrode/reducing the coated-film thickness for silicon active materials are many effective techniques to solve the above-mentioned problems<sup>25</sup>. However, the complicated fabrication processes of these above Si-based electrodes may hinder their large-scale production. It is still a severe challenge to achieve high-performance silicon electrodes using a low-cost/facile route.

Up to now, great attentions have been paid to explore the potential applications of promising Si-based electrodes for lithium-ion battery. Yu et al. synthesized 3D porous Si anodes by a magnesiothermic reduction approach, showing their good cycling stability (reversible capacity of 2600 mAh g<sup>-1</sup> over 100 cycles)<sup>26</sup>. Nam et al. produced carved Si electrodes using the laser interference lithography (LIL) technique under controlled exposure conditions. These electrodes exhibited a superior Li storage capacity and a high rate capability<sup>27</sup>. Wu et al. reported a SiNP@CT via electrospinning methods, revealing these electrodes presented long cycle life (200 cycles with 90% capacity retention) and good rate capability<sup>28</sup>. Magasinski et al. described a Si-C nano-composite granule using chemical vapor deposition (CVD) process. These materials delivered high capacity (1500 mAh g<sup>-1</sup>) at 1 C and excellent rate capability (approximately 1000 mAh g<sup>-1</sup> at a high rate of 8 C)<sup>29</sup>. Even though the

SUBJECT AREAS:

BATTERIES

NANOWIRES

ELECTRONIC MATERIALS

ENVIRONMENTAL CHEMISTRY

Received

22 February 2013

Accepted

26 March 2013

Published

9 April 2013

Correspondence and requests for materials should be addressed to C.W.Z. (chongwuz@usc.edu) or G.Z.S. (gzshen@semi.ac.cn)

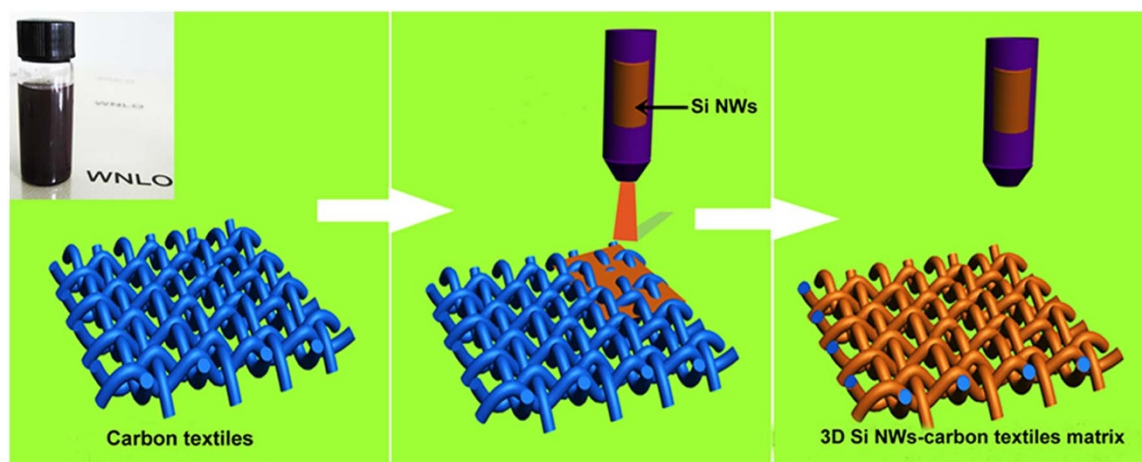


**Figure 1** | Schematic illustration of the formation of hierarchical silicon-carbon textiles matrix. A complete route is composed of Si-based-ink preparation, spray-coating operation, and thermal treatment.

inspiring results in terms of cycling life and rate capability of these electrodes have been obtained, no information about across-the-board performances (large energy density, high power density, enhanced battery stability, and satisfying safety) in single complete Si-based storage unit was disclosed. Only in this unit can we principally replace existing graphite anodes with better comprehensive performance silicon-based electrodes.

Herein, we first report a novel matrix of hierarchical Si nanowires (NWs)-carbon textiles matrix as a binder-free electrode via a facile route. Full Si NWs anodes/commercial  $\text{LiCoO}_2$  cathodes

batteries were successfully assembled in order to investigate their corresponding comprehensive performances. These unique Si/carbon textiles scaffold electrodes could enhance the electric conductivity and stabilize the whole structure, leading to their enhanced specific capacity ( $2950 \text{ mAh g}^{-1}$  at  $0.2 \text{ C}$ ), good repeatability/rate capability (even  $>950 \text{ mAh g}^{-1}$  at high rate of  $5 \text{ C}$ ), long cycling life, and excellent stability in various external conditions including curvature, temperature, and humidity. We provide a possibility to replace commercial graphite material with superior performance Si-based matrix.

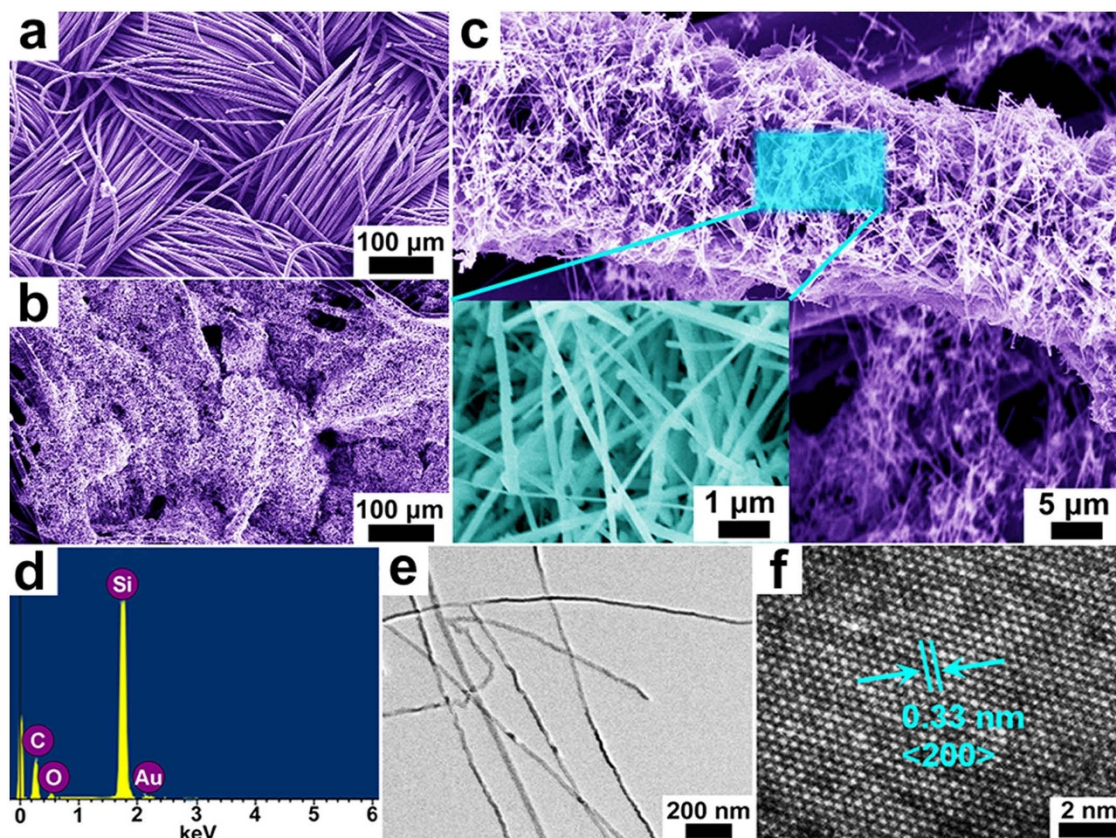


**Figure 2** | Morphological and structural analysis of hierarchical Si nanowires-carbon textiles matrix. (a, b) Typical SEM images of samples/carbon textiles composites. (c) SEM image of a single carbon microfiber uniformly coated with Si nanowires. The EDX spectrum (d), the TEM image (e), and HR-TEM image (f) of the resulting materials.



## Results

**Fabrication and characterization of as-prepared silicon-carbon composites.** Figure 1 shows the fabrication processes of Si NWs-carbon textiles composites. Briefly, the Si NWs were dissolved in ethanol solution to achieve a homogeneous suspension, as shown in Figure 1 inset. Then, carbon textiles were gradually coated with as-synthesized Si NWs during the fabricating process, where we can see a layer of our samples attached tightly to the carbon textiles. Finally, hierarchical Si NWs-carbon textiles anodes were achieved after thermal treatment for them. More details have been explained in Methods section.

The SEM image of pure carbon textiles with smooth surfaces before coating is shown in Figure 2a and Supplementary Figure S1, which clearly illustrates their well-established texture structures and each carbon microfiber with uniform diameter of approximately 10  $\mu\text{m}$ . For comparison, Figure 2b shows the FESEM image of novel samples/carbon textiles matrix. It can be seen that the carbon textiles coated with resulting materials still keep its original cloth-like feature, illustrating good mechanical-strength of this substrate. Typical SEM image of the single silicon-carbon composite fiber from this above matrix demonstrates numerous uniform silicon nanowires with length of  $\sim 10 \mu\text{m}$  stuck tightly to the surface of single carbon microfiber, as shown in Figure 2c. Figure 2c inset shows a higher-magnification SEM image of the samples, illustrating the diameter of these Si NWs with about 30–50 nm.

The distributions of Si and C are also shown in Supplementary Figure S2, revealing a uniform distribution of Si and C through the whole matrix (in the SEM image area marked with an orange square). The EDX spectrum collected from the surface part of Si samples on carbon textiles (Fig. 2d) is consistent well with the above mapping

results. The TEM image of Si NWs is shown in Figure 2e, the diameters of these samples are approximately 30 nm. The high-resolution TEM (HRTEM) image shown in Figure 2f reveals the interplanar spacing of  $\sim 0.33 \text{ nm}$ , corresponding to the  $\langle 200 \rangle$  plane of single-crystalline Si material.

**Electrochemical characterizations of coin-type half-cells and full Li-ion batteries based on Si NWs-carbon textiles matrix as a binder-free anode.** Electrochemical measurements of as-prepared Si NWs-carbon textiles electrodes were performed in coin-type half-cells at the room temperature. Figure 3a and 3b shows voltage profiles of Si NWs-carbon textiles electrodes cycled between 0.01–1.5 V at 0.2 C and 1 C for 1st, 2nd, 10th, 100th, and 200th cycles, respectively. Both first discharge curves (0.2 C and 1 C) present the flat plateaus at  $\sim 0.25 \text{ V}$ , which corresponds to the lithiation process of crystalline Si to form amorphous  $\text{Li}_x\text{Si}$  phase and the formation of typical solid electrolyte interphase (SEI)<sup>30,31</sup>. Afterwards, the profiles of following charge-discharge curves almost remain the same for 200 cycles. Figure 2c demonstrates the charge/discharge curves of Si NWs-carbon textiles anodes at 0.2 C for 200 cycles. The reversible specific capacity of as high as  $2950 \text{ mAh g}^{-1}$ , 92% of the initial value after 200 cycles is obtained, which reveals their corresponding excellent cyclability. Furthermore, the coulombic efficiency (CE) of these Si-based electrodes is approximately 99.6%, indicating highly efficient lithium insertion/extraction. In Figure 4d, we can clearly observe the specific capacities still remain 1500 and  $1100 \text{ mAh g}^{-1}$  after 200 cycles when the Si electrodes were cycled at the rates of 1 C and 4 C, respectively, proving their wonderful rate capabilities by introducing this novel hybrid structures. Moreover, the CE at rates of 1 C and 4 C approach 99.5%, revealing the cycling stability of this Si

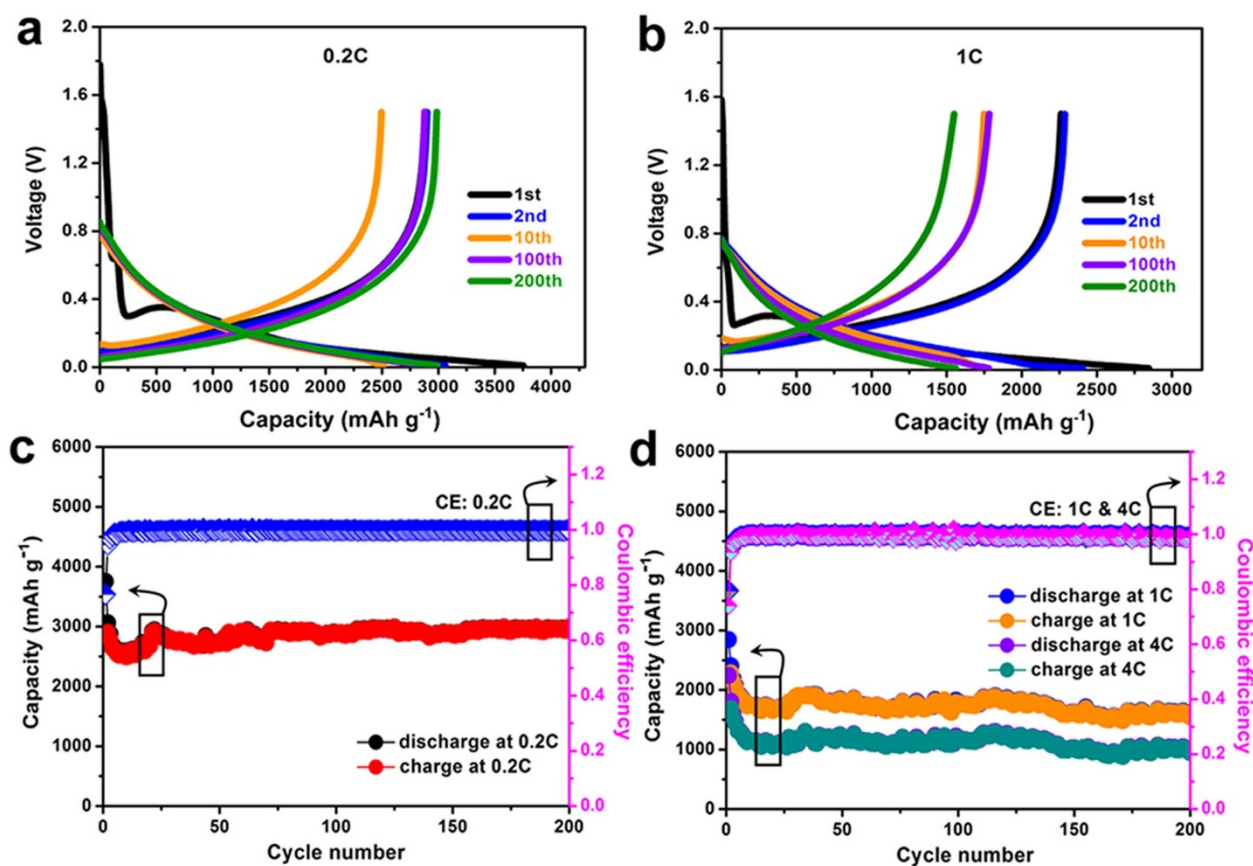


**Figure 3 | Electrochemical characterizations of Si-based half-cells.** (a, b) Voltage profiles of as-prepared Si NWs-carbon textiles electrodes between 0.01–3.0 V at rates of 0.2 C and 1 C. (c) Cycling performance of these electrodes at 0.2 C and their corresponding coulombic efficiency. (d) The rate capability of these electrodes cycled at rates of 1 C and 4 C for as high as 200 cycles.

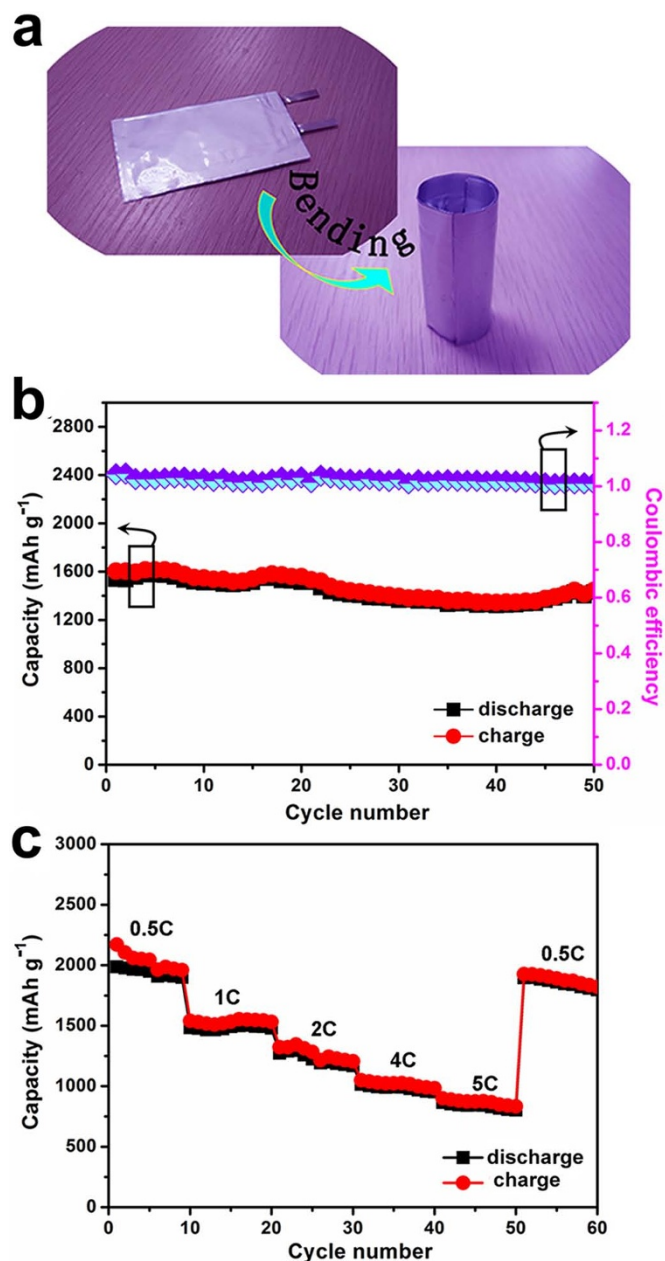


**Figure 4 | Electrochemical properties of Si-based full batteries.** (a) Photograph of full Si-based lithium-ion battery under non-bending and bending. (b) Cycling performance of the non-bending Li-ion batteries based on silicon electrodes cycled at 1 C for 50 cycles and their CE. (c) Their corresponding rate capability cycled at various rates of 0.5 C, 1 C, 2 C, 4 C, and 5 C for total 60 cycles.

NWs-carbon textiles matrix during charge/discharge process. Also, galvanostatic discharge profiles were also investigated by comparing the batteries with samples/carbon textiles and carbon textiles only, as shown in Supplementary Figure S3. It can be seen that the negligible capacity of the pure carbon textiles based device, reveals that the total capacity is primarily attributed to that of the loaded silicon materials<sup>32–34</sup>. All these results reveal that lithium-ion batteries based on as-fabricated silicon anodes could indicate superior electrochemical activities.

To investigate the practical applications of the Si-based electrodes, we described a novel designed full battery formed by combining a high capacity silicon-carbon anode with a high voltage of commercial LiCoO<sub>2</sub> cathode. A full Si-based anodes/LiCoO<sub>2</sub> cathodes battery

was assembled and then evaluated by galvanostatic cycling at various C-rates. The capacities of cathode (LiCoO<sub>2</sub>) and anode (Si) are approximately 10 ~ 12 and 2.1 ~ 3.4 mAh, respectively. Therefore, it's worth mentioning that these LiCoO<sub>2</sub> cathodes are just regarded as counter electrodes and the as-assembled full batteries are anode-limited units and 1 C rate referring to the anode weight is 4200 mAh g<sup>-1</sup><sup>33,35,36</sup>. Figure 4a displays a bending assembled battery rolled into a cylinder, which illustrates its outstanding flexibility. Figure 4b shows cycle performance and corresponding CE of these non-bending full Si NWs/LiCoO<sub>2</sub> batteries at 1 C between 2.5–4.0 V over 50 cycles, from which we can see that these electrodes can deliver enhanced reversible specific capacity (as high as 1580 mAh g<sup>-1</sup>) with high CE (approximately 99.7%). Further, we investigated the corresponding rate capability with the various rates stepwise increased from 0.5 C to 5 C and then switched back, as shown in Figure 4c. Although such a high 5 C (21 A g<sup>-1</sup>) was imposed on these electrodes, their corresponding specific capacities were still as high as 950 mAh g<sup>-1</sup>. The stability to maintain a large capacity at various high rates for Si anodes can be attributed to the novel Si NWs-carbon textiles matrix, facilitating improved electric conductivity, fully accessible interior, and fast lithiation and delithiation reactions for the total Si-based architecture.

For the increasing demands of the future electronic modules with multiple functional requirements, such as portability, transparency, flexibility, and wear-ability, we designed the novel flexible full lithium-ion batteries based on Si NWs-carbon textiles. The plot of self-discharge characteristic of the flexible batteries is illustrated in Figure 5a. The voltage value remains at ~3.25 V over 360 h at the room temperature, revealing the low self-discharge performance and stable energy storage systems. Further, we investigated the impact of both tensile and compressive stress for the device along its vertical direction. Figure 5b reveals that the average voltage displays no significant change under both tensile/compressive bending states between 20° and 80°. Similarly, the voltage of the device remains stable during the 160 folded cycles. Compared with the battery at no-bending state (Fig. 5d), the voltage can still keep as high as 3.24 V, even though the battery has been bent severely (Fig. 5e). More details have been added in Supplementary Video S1. All these results vividly prove low self-discharge property, high flexibility, and excellent stability of the as-assembled lithium ion batteries.

The essential performances of the as-assembled full battery were further performed with various temperature (T) and humidity (H) parameters. As shown in Figure 6a, the voltage values of the full lithium-ion batteries with the change of time are hardly affected by the change of temperature, showing as-fabricated batteries achieve the highly stable capability. Figure 6b shows the reversible capacities of Si NWs-carbon textiles anodes cycled at 1 C. The discharge capacities decline from 1700 to 1300 mAh g<sup>-1</sup> with the ambient temperature decreased from 45°C to 10°C, which is a common phenomenon that the capacities of lithium-ion batteries can be affected by ambient temperature. When the temperature finally returns to 45°C, the initial capacity value of 1680 mAh g<sup>-1</sup> can be recovered, revealing the stable electrochemical activity of this Li-ion battery under varied ambient temperature. Similarly, the stable feature of the cell devices at the different humidity (50%, 70%, and 90%) was also performed in this Chamber. Even though humidity is continuously raised from 50% to 90%, the voltage of a full lithium-ion battery always maintains at ~3.7 V, as shown in Figure 6c. The discharge capacities can remain a stable cyclable stage during 30 cycles at the different humidity, as illustrated in Figure 6d. These results exhibit the perfect stability, reversibility, and cyclability of our full Si/LiCoO<sub>2</sub> batteries when applying in the special conditions.

**Display of these full Si-based Li-ion batteries.** Because of the advantages identified above, these full lithium-ion batteries hold the potential to supply power for promising applications. For

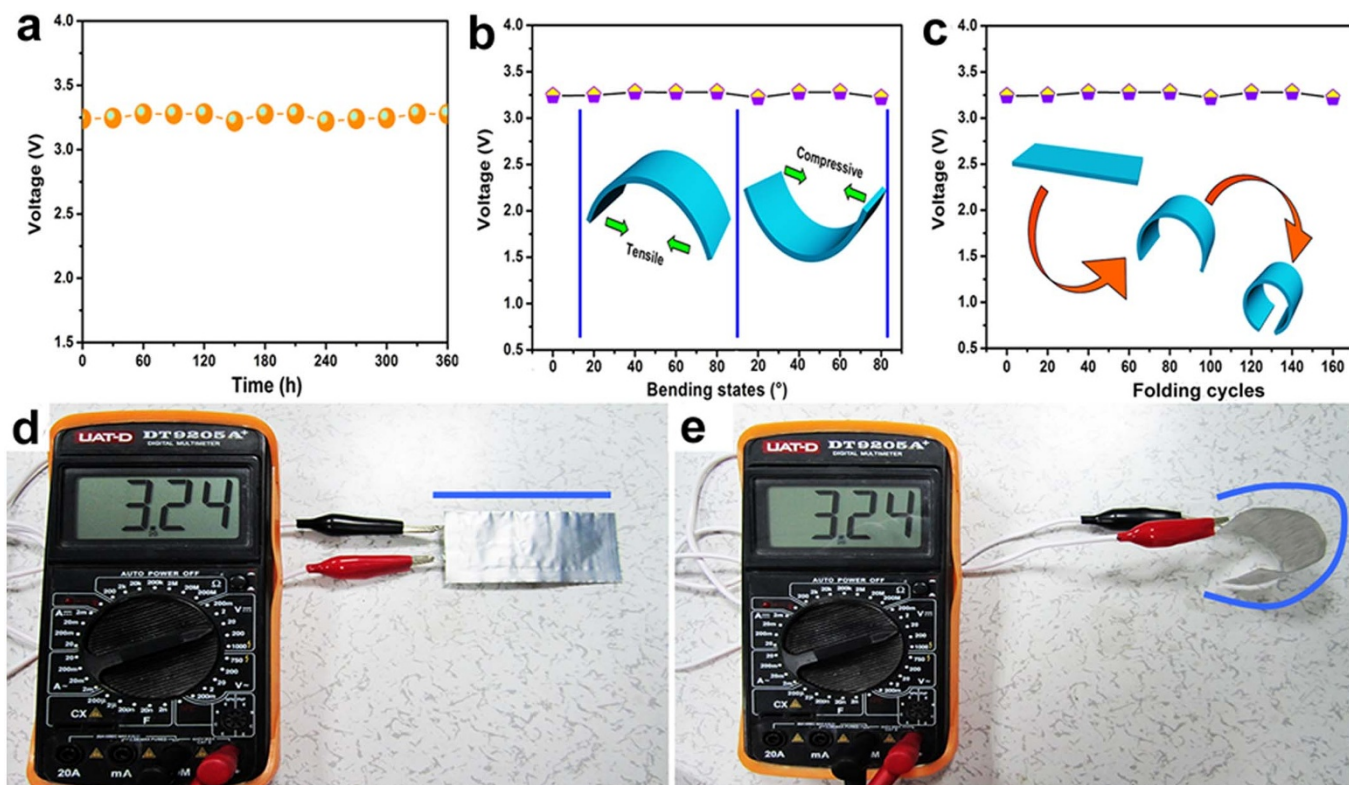


**Figure 5** | Stability measurements of self-discharging and curvature situations for as-assembled batteries. (a) Self-discharge characterization of full Si NWs-carbon textiles/LiCoO<sub>2</sub> lithium-ion batteries. (b, c) Voltage profiles of these flexible full lithium-ion batteries for bending states. (d, e) The voltage retention test of this battery under non-bending and bending.

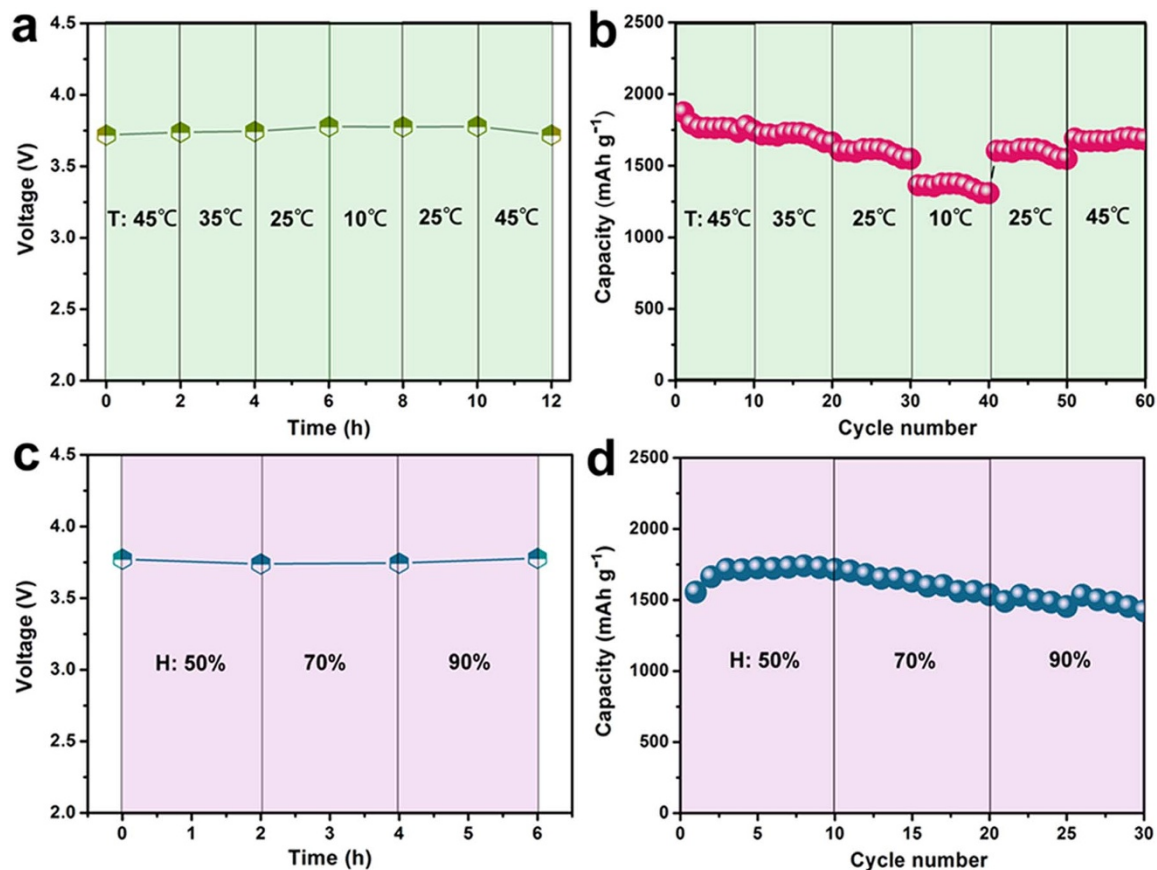


**Figure 6** | Stability tests of full lithium-ion batteries under various temperature and humidity. The as-fabricated batteries were measured at various temperature of 10, 25, 35, and 45°C and various humidity of 50, 70, and 90%, respectively.

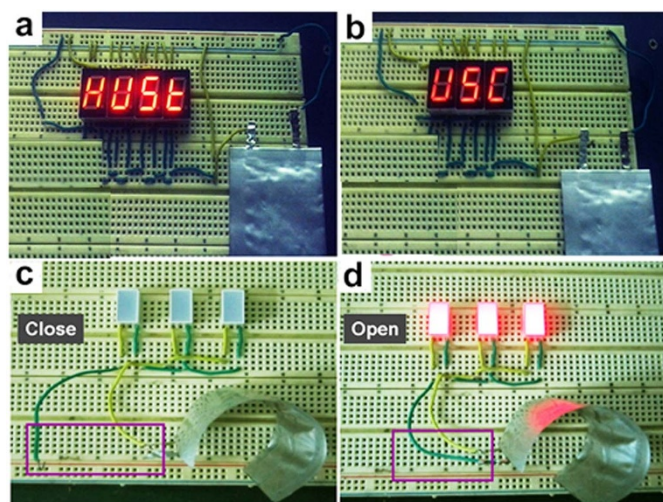


**Figure 7 | Display.** (a,b) The photographs of “HUST” and “USC” patterns lightened by an as-assembled lithium-ion battery (the initials of Huazhong University of Science and Technology & University of Southern California). (c,d) Optical images of three red LEDs driven by a full battery like a Close/Open switch.

example, two rows of nixietubes showing red visible patterns of “HUST” (Fig. 7a) and “USC” (Fig. 7b), respectively, can be successfully driven by an as-fabricated battery. More importantly, the battery can light three LED devices when the battery is used to start supplying power, as shown in Figure 7c and 7d. The brightness of devices is almost unaffected performance under greatly bending state so that the lithium-ion battery is believed to meet future portable, flexible, and ultrathin energy storage system options.

## Discussion

The above obtained superior electrochemical properties of the as-fabricated hierarchical Si NWs-carbon textiles electrodes are not simply a result of the mixture of the two units (Si & C). It is expected that these performance advancements may originate from the synergistic effect of the efficient integration of the respective advantages from both Si and C individual units in a complete cell configuration. This matrix design with the worthwhile merits achieved by combining high-capacity silicon anodes with high-conductivity carbon textiles provides several unique features: (i) the numerous 1D Si nanowires are beneficial to the insertion/extraction of  $\text{Li}^+$  among them, which also shorten the charge transfer expressway and lower the exchange resistance for lithium ions between active functional materials and electrolyte; (ii) the Si nanowires coated on carbon textiles with many spaces among them have an increased portion of exposed surfaces, which facilitates lithium-ion/electron transport inside active materials and diffusion of the electrolyte in a short time for fast energy storage; (iii) the current silicon nanowires/carbon textiles matrix can obtain outstanding electronic conductivity because of many Si nanowires tightly attached to the C substrate to form very good adhesion and electrical contact. Herein, it can be concluded that the essential performances of Si-based anodes can be indeed improved by designing the novel hierarchical network matrix.

Considering various desired persistent stability of our demonstrated electrodes during electrochemical processes, we reveal that the spray-coating method with simple, rapid, and low-cost features could keep the good adhesiveness between active materials and substrates due to electrostatic force effect among them, nano-scale raw inks, and special fabricated procedures. Therefore, this is an efficient way to fulfill large-scale industrialization of future critical Li-ion

batteries based on high-performance Si anodes by introducing desired spray-coating technique.

In summary, we first report the unique matrix of hierarchical Si NWs-carbon textiles electrodes with high capacity ( $2950 \text{ mAh g}^{-1}$  at  $0.2 \text{ C}$ ), long cycle life (as long as 200 cycles), good rate capability, and excellent stability with different temperature, humidity, and curvature. Their corresponding superior across-the-board performances can provide the great possibility to replace the defective graphite anodes with Si-based material as a promising anode. Furthermore, this strategy to fabricate novel Si-based/3D carbon template hybrid matrix via a facile spray-coating approach can be extended to fabricating other high-performance composite electrodes for energy storage units. As-assembled Si-based lithium ion batteries hold the great potential power for the next-generation functionalities, such as optoelectronic devices, portable/curvilinear electronics, sustainable electric vehicles, etc.

## Methods

**Synthesis of hierarchical silicon nanowires-carbon textiles matrix.** Firstly, silicon nanowires were synthesized via a CVD method. Briefly, the CVD process was carried out at  $450^\circ\text{C}$  for 28 min under  $\text{SiH}_4$  (111 sccm) and  $\text{H}_2$  (20 sccm) mixed gas. The chamber in tube furnace was cooled down automatically in the atmosphere and then silicon was obtained. After, these Si nanowires were mixed with 40% HF water/ethanol (1 : 1, v/v) solution (40 ml). The Si NWs solution was ultrasonically agitated by using a sonicator and then centrifuged at  $6000 \text{ r min}^{-1}$  for 2 min to separate the stable suspension of Si nanoparticles and the aggregation of Si nanoparticles, which were collected and redispersed in ethanol with sonication, respectively. These same steps were repetitively proceeded at 3 times and then as-obtained Si nanoparticles were dried under vacuum at  $80^\circ\text{C}$  for 4 h. Finally, 50 mg of the as-dried Si samples were also immersed in ethanol (10 mL) with sonication for 30 min, forming a homogeneous Si NWs-based solution. The cleaned carbon textiles were gradually coated with the Si NWs slurry. The Si/carbon textiles composites were heated at  $300^\circ\text{C}$  under high-purity  $\text{N}_2$  atmosphere for 30 min to enhance the soundness between silicon and carbon-substrate. Finally, 3D Si NWs-carbon textiles matrix was achieved via a facile spray-coating approach.

**Sample characterization.** The as-prepared Si NWs-carbon textiles samples were characterized with field emission scanning electron microscopy (FE-SEM, FEI Quanta 450), and transmission electron microscopy (TEM; JEOL JEM-2010 HT).

**Electrochemical evaluation.** For half-cells assembly, electrochemical experiments were performed using CR2032-type coin cells with Celgard 2400 as the separator and lithium foil as counter electrode. The electrolyte was 1 M  $\text{LiPF}_6$  in the mixture of ethylene carbonate (EC) and diethyl carbonate (DEC) (1 : 1 in volume ratio). The working electrodes were binder-free Si NWs-carbon textiles matrix. The mass of Si NWs deposited on carbon textiles substrate was determined by weighing the substrate before and after fabricating process. The loading density of the silicon samples is calculated as  $2.4\text{--}3.5 \text{ mg cm}^{-2}$ . Similarly, as-assembled full flexible Li-ion battery was composed of Si NWs-carbon textiles anode, commercial  $\text{LiCoO}_2$  cathode, Celgard 2400 separator, and  $\text{LiPF}_6$ -based electrolyte. The coin cells and full lithium-ion batteries were assembled in an argon-filled glove box where oxygen and water concentration were strictly limited to below 1 ppm. The galvanostatic cycling measurements were performed on LAND battery testing system. The tests of the devices at various temperature and humidity were carried out in Temp & Humi Programmable Chamber.

1. Ellis, B. L. *et al.* A multifunctional 3.5 V iron-based phosphate cathode for rechargeable batteries. *Nat. Mater.* **6**, 749–753 (2007).
2. Ji, H. X. *et al.* Ultrathin graphite foam: a three-dimensional conductive network for battery electrodes. *Nano Lett.* **12**, 2446–2451 (2012).
3. Wang, H. G., Ma, D. L., Huang, X. L., Huang, Y. & Zhang, X. B. General and controllable synthesis strategy of metal oxide/ $\text{TiO}_2$  hierarchical heterostructures with improved lithium-ion battery. *Sci. Rep.* **2**, 701 (2012).
4. Lee, K. T. & Cho, J. Roles of nanosize in lithium reactive nanomaterials for lithium ion batteries. *Nano Today* **6**, 28–41 (2011).
5. Xia, X. H. *et al.* Integrated Photoelectrochemical Energy Storage: Solar Hydrogen Generation and Supercapacitor. *Sci. Rep.* **2**, 981 (2012).
6. Chen, T. *et al.* A integrated “energy wire” for both photoelectric conversion and energy storage. *Angew. Chem. Tnt. Ed.* **51**, 11977–11980 (2012).
7. Jia, H. P. *et al.* Novel three-dimensional mesoporous silicon for high power lithium-ion battery anode material. *Adv. Energy Mater.* **1**, 1036–1039 (2011).
8. Du, N. *et al.* Porous  $\text{Co}_3\text{O}_4$  nanotubes derived from  $\text{Co}_4(\text{CO})_{12}$  clusters on carbon nanotube templates: a highly efficient material for Li-battery applications. *Adv. Mater.* **19**, 4505–4509 (2007).
9. Wang, H. L. *et al.* Rechargeable  $\text{Li-O}_2$  batteries with a covalently coupled  $\text{MnCo}_2\text{O}_4$ -graphene hybrid as an oxygen cathode catalyst. *Energy Environ. Sci.* **5**, 7931–7935 (2012).



10. Chan, C. K. *et al.* High-performance lithium battery anodes using silicon nanowires. *Nat. Nanotechnol.* **3**, 31–35 (2008).
11. Hertzberg, B., Alexeev, A. & Yushin, G. Deformations in Si-Li anodes upon electrochemical alloying in nano-confined space. *J. Am. Chem. Soc.* **132**, 8548–8549 (2010).
12. Cui, Y. & Lieber, C. M. Functional nanoscale electronic devices assembled using silicon nanowire building blocks. *Science* **291**, 851–853 (2001).
13. Chen, P. C., Xu, J., Chen, H. T. & Zhou, C. W. Hybrid silicon-carbon nanostructured composite as superior anodes for lithium ion batteries. *Nano Res.* **4**, 290–296 (2011).
14. Zhang, G. Q., Yu, L., Wu, H. B., Hoster, H. E. & Lou, X. W. Formation of ZnMn<sub>2</sub>O<sub>4</sub> ball-in-ball hollow microspheres as a binder-free anode for lithium-ion batteries. *Adv. Mater.* **24**, 4609–4613 (2012).
15. Zhou, X. S., Cao, A. M., Wan, L. J. & Guo, Y. G. Spin-coated silicon nanopaticles/graphene electrode as a binder-free anode for high-performance lithium-ion batteries. *Nano Res.* **5**, 845–853 (2012).
16. Kim, H., Seo, M., Park, M. H. & Cho, J. A critical size of silicon nano-anodes for lithium rechargeable batteries. *Angew. Chem. Int. Ed.* **49**, 2146–2149 (2010).
17. Yao, Y. *et al.* Highly conductive, mechanically robust, and electrochemical inactive TiC/C nanofiber scaffold for high-performance silicon anode batteries. *ACS NANO* **5**, 8346–8351 (2011).
18. Ge, M. Y., Rong, J. P., Fang, X. & Zhou, C. W. Porous doped silicon nanowires for lithium ion battery anode with long cycle life. *Nano Lett.* **12**, 2318–2323 (2012).
19. Chen, H. T. *et al.* Bulk synthesis of crystalline and crystalline core/amorphous shell silicon nanowires and their application for energy storage. *ACS NANO* **5**, 8383–8390 (2011).
20. McDowell, M. T. & Cui, Y. Single nanostructure electrochemical devices for studying electronic properties and structural changes in lithiated Si nanowires. *Adv. Energy Mater.* **1**, 894–900 (2011).
21. Li, H., Wang, Z. X., Chen, L. Q. & Huang, X. J. Research on advanced materials for Li-ion batteries. *Adv. Mater.* **21**, 4593–4607 (2009).
22. Golmon, S., Maute, K., Lee, S. H. & Dunn, M. L. Stress generation in silicon particles during lithium insertion. *Appl. Phys. Lett.* **97**, 033111 (2010).
23. Obrovac, M. N. & Krause, L. J. Reversible cycling of crystalline silicon powder. *J. Electrochem. Soc.* **154**, A103–A108 (2007).
24. Li, J. C., Dozier, A. K., Li, Y. C., Yang, F. Q. & Cheng, Y. T. Crack pattern formation in thin film lithium-ion battery electrodes. *J. Electrochem. Soc.* **158**, A689–A694 (2011).
25. He, Y., Yu, X. Q., Wang, Y. H., Li, H. & Huang, X. J. Alumina-coated patterned amorphous silicon as the anode for a lithium-ion battery with high coulombic efficiency. *Adv. Mater.* **23**, 4938–4941 (2011).
26. Yu, Y. *et al.* Reversible storage of lithium in silver-coated three-dimensional macroporous silicon. *Adv. Mater.* **22**, 2247–2250 (2010).
27. Nam, S. H. *et al.* Probing the lithium ion storage properties of positively and negatively carved silicon. *Nano Lett.* **11**, 3656–3662 (2011).
28. Wu, H. *et al.* Engineering empty space between Si nanoparticles for lithium-ion battery anodes. *Nano Lett.* **12**, 904–909 (2012).
29. Magasinski, A. *et al.* High-performance lithium-ion anodes using a hierarchical bottom-up approach. *Nat. Mater.* **9**, 353–358 (2010).
30. McDowell, M. T. *et al.* Studying the kinetics of crystalline silicon nanoparticle lithiation with in situ transmission electron microscopy. *Adv. Mater.* **24**, 6034–6041 (2012).
31. Kim, H. & Cho, J. Superior lithium electroactive mesoporous Si@carbon core-shell nanowires for lithium battery anode material. *Nano Lett.* **8**, 3688–3691 (2008).
32. Luo, Y. S. *et al.* Seed-assisted synthesis of highly ordered TiO<sub>2</sub>@ $\alpha$ -Fe<sub>2</sub>O<sub>3</sub> core/shell arrays on carbon textiles for lithium-ion battery applications. *Energy Environ. Sci.* **5**, 6559–6566 (2012).
33. Wang, X. H. *et al.* Nanostructured NiO electrode for high rate Li-ion batteries. *J. Mater. Chem.* **21**, 3571–3573 (2011).
34. Liu, B. *et al.* Hierarchical three-dimensional ZnCo<sub>2</sub>O<sub>4</sub> nanowire arrays/carbon cloth anodes for a novel class of high-performance flexible lithium-ion batteries. *Nano Lett.* **12**, 3005–3011 (2012).
35. Armstrong, G., Armstrong, A. R., Bruce, P. G., Reale, P. & Scrosati, B. TiO<sub>2</sub>(B) nanowires as an improved anode material for lithium-ion batteries containing LiFePO<sub>4</sub> or LiNi<sub>0.5</sub>Mn<sub>1.5</sub>O<sub>4</sub> cathodes and polymer electrolyte. *Adv. Mater.* **18**, 2597–2600 (2006).
36. Hassoun, J., Lee, K. S., Sun, Y. K. & Scrosati, B. An advanced lithium ion battery based on high performance electrode materials. *J. Am. Chem. Soc.* **133**, 3139–3143 (2011).

## Acknowledgments

This work was supported by the National Natural Science Foundation (51002059, 21001046, 91123008), the 973 Program of China (2011CB933300), the Program for New Century Excellent Talents of the University in China (grant no. NCET-11-0179) and the Natural Science Foundation of Hubei Province (2011CDB035). Special thanks to the Analytical and Testing Center of HUST and the Center of Micro-Fabrication and Characterization (CMFC) of WNLO for using their facilities.

## Author contributions

B.L., G.Z.S., D.C., Y.B.C. and C.W.Z. devised the original concept, designed the experiments, discussed the interpretation of results and co-wrote the paper. B.L. performed the electrochemical experiments. H.T.C. supported the CVD synthesis. All authors discussed the results and participated in manuscript revision.

## Additional information

**Supplementary information** accompanies this paper at <http://www.nature.com/scientificreports>

**Competing financial interests:** The authors declare no competing financial interests.

**License:** This work is licensed under a Creative Commons Attribution-NonCommercial-NoDerivs 3.0 Unported License. To view a copy of this license, visit <http://creativecommons.org/licenses/by-nc-nd/3.0/>

**How to cite this article:** Liu, B. *et al.* Hierarchical silicon nanowires-carbon textiles matrix as a binder-free anode for high-performance advanced lithium-ion batteries. *Sci. Rep.* **3**, 1622; DOI:10.1038/srep01622 (2013).